Neurobiology of Pain 9 (2021) 100060

Contents lists available at ScienceDirect

Neurobiology of Pain

journal homepage: www.sciencedirect.com/journal/neurobiology-of-pain

Parabrachial complex processes dura inputs through a direct trigeminal ganglion-to-parabrachial connection

Olivia Uddin [a], Michael Anderson [a], Jesse Smith [a], Radi Masri [b], Asaf Keller [a,*]

[a] Department of Anatomy and Neurobiology, Program in Neuroscience, University of Maryland School of Medicine, Baltimore, MD 21201, United States
[b] Department of Advanced Oral Sciences and Therapeutics, University of Maryland School of Dentistry, Baltimore, MD 21201, United States

ARTICLE INFO

Keywords:
Pain
Migraine
Parabrachial
Trigeminal

ABSTRACT

Migraines cause significant disability and contribute heavily to healthcare costs. Irritation of the meninges' outermost layer (the dura mater), and trigeminal ganglion activation contribute to migraine initiation. Maladaptive changes in central pain-processing regions are also important in maintaining pain. The parabrachial complex (PB) is a central region that mediates chronic pain. PB receives diverse sensory information, including a direct input from the trigeminal ganglion. We hypothesized that PB processes inputs from the dura. Using *in vivo* electrophysiology recordings from single units in anesthetized rats we identified 58 neurons in lateral PB that respond reliably and with short latency to electrical dura stimulation. After injecting tracer into PB, anatomical examination reveals retrogradely labeled cell bodies in the trigeminal ganglion. Neuroanatomical tract-tracing revealed a population of neurons in the trigeminal ganglion that innervate the dura and project directly to PB. These findings indicate that PB is strategically placed to process dura inputs and suggest that it is directly involved in the pathogenesis of migraine headaches.

1. Introduction

Migraines are a highly prevalent condition involving recurrent severe headaches. These disrupt daily activities and significantly contribute to healthcare burden (Headache Classification Committee of the International Headache Society (IHS), 2018; Burch et al., 2018). Migraine headaches are often accompanied by autonomic instability, photophobia, phonophobia and sensitivity to normally innocuous tactile or thermal stimuli (allodynia) (Burstein et al., 2000). Allodynia impacts a significant proportion of migraine patients (Bigal, 2008) and is a predictor of poor treatment response and migraine chronification (Burstein et al., 2004; Lipton, 2017; Louter, 2013).

A number of mechanisms have been identified as likely contributors to migraines (Noseda and Burstein, 2013; Dodick, 2018). A key anatomical substrate in migraine pain is the trigeminal system that relays sensory information, including pain, from the face and head region. The outermost layer of the meninges, the dura mater, is innervated by sensory afferents of neurons in the trigeminal ganglion. Dura manipulation in humans during neurosurgery is often painful (Fontaine, 2018) and dura irritation is considered an initiating factor in migraine (Moskowitz, 1984). In rodents, dura irritation models migraine-like symptoms (Burgos-Vega, 2019; Oshinsky and Gomonchareonsiri, 2007).

The parabrachial complex (PB) is a bilateral midbrain structure that plays important roles in pain processing, as well as many survival-related homeostatic and interoceptive functions (Davern, 2014; Martelli et al., 2013; Hajnal et al., 2009; Campos et al., 2018; Chiang, 2019). PB's anatomical connections place it in an ideal position to modulate pain. It receives direct spinal inputs from the trigeminal nucleus and dorsal horn (Gauriau and Bernard, 2002; Spike et al., 2003; Saito, 2017) and communicates with regions important for sensory and emotional processing (Gauriau and Bernard, 2002; Krukoff et al., 1993; Bianchi et al., 1998; Roeder, 2016). Amplified activity of PB neurons is causally related to chronic pain (Jergova et al., 2008; Matsumoto et al., 1996; Uddin, 2018; Raver, 2020) and changes in PB activity contribute even more heavily in models of craniofacial and orofacial pain (Rodriguez, 2017). Significantly, there exists a direct connection from trigeminal ganglion neurons to PB (Rodriguez, 2017; Panneton et al., 2006; Cavanaugh, 2011a, 2011b; Panneton and Gan, 2014); bypassing the canonical node in the spinal trigeminal nucleus. Thus, PB is strategically placed to process dura inputs, and to be involved in the pathophysiology of migraine.

Here, we test the hypothesis that PB processes inputs from the dura.

Abbreviations: PB, parabrachial complex; TG, trigeminal ganglion; CTB, cholera Toxin B; FG, FluoroGold.

* Corresponding author at: 20 Penn Street, Baltimore, MD 21201, United States.
E-mail address: akeller@som.umaryland.edu (A. Keller).

https://doi.org/10.1016/j.ynpai.2021.100060
Received 27 October 2020; Received in revised form 18 December 2020; Accepted 17 January 2021
Available online 21 January 2021

2. Methods

2.1. Animals

All procedures were conducted according to Animal Welfare Act regulations and Public Health Service guidelines and approved by the University of Maryland School of Medicine Animal Care and Use Committee. Twenty-two male and female Wistar rats (Envigo, Indianapolis, IN, or bred in-house), ages 3–12 months, contributed to the electrophysiology data presented here. For anatomical tracing studies, we used 5 Wistar rats (3 female, 2 male) ages 3–6 months.

2.2. Electrophysiology preparation

We anesthetized (Level III-2, as defined by (Friedberg et al., 1999) all rats with 20% urethane in sterile saline. Rats were placed in a stereotaxic frame with a heating pad to maintain body temperature. We made a small craniotomy over the recording site to target PB (AP −9.2 and ML +1.9, relative to bregma, and DV −6.0 mm, relative to dura surface). We exposed the dura mater, over the middle meningeal artery, for stimulation.

2.3. In vivo electrophysiology

Using platinum-iridium recording electrodes (2–4 MΩ) produced in our laboratory, we recorded from the PB both contralateral and ipsilateral to dura stimulation site. We isolated units responsive to electrical dura stimulation and digitized the waveforms using a Plexon acquisition system (Plexon Inc., Dallas, TX).

2.4. Identification of dural stimulus-responsive neurons

We used bipolar platinum-iridium electrodes to electrically stimulate the dura with the goal of identifying PB neurons that process dura inputs. We positioned these electrodes over the middle meningeal artery, either contralateral or ipsilateral to the site of PB recording. Electrical stimulation parameters were 1–3 mA intensity, 800–850 μs duration, 0.3 Hz, chosen based on prior reports (Burstein et al., 1998; Strassman et al., 1996) and preliminary recordings showing that these stimulus parameters were optimal in eliciting reliable PB responses. To define dura stimulus-responsive neurons, we used NeuroExplorer (Plexon Inc, Dallas, TX) to construct peristimulus time histograms (PSTHs), and cells that fired with greater than 95% confidence in the first 100 ms after stimulation were considered responsive to dura stimulation.

2.5. Histological confirmation of recording site

To confirm the location of recorded neurons we made electrolytic lesions at the conclusion of recording experiments. Animals were perfused transcardially with 0.05 M phosphate buffered saline, followed by 4% paraformaldehyde (PFA). Brains were extracted and incubated overnight in 4% PFA at room temperature. We then sliced brains coronally into 70 to 80 μm thick sections and stained them with Toluidine Blue.

2.6. Electrophysiology data analysis

Cells were sorted using Offline Sorter (Plexon) using dual thresholds and principal component analysis. We calculated spontaneous mean firing rates using NeuroExplorer, and used a custom MATLAB (MathWorks, Natick, MA) script to quantify responses to electrical stimulation of the dura. Responsive neurons were defined as units with activity that exceeded the 95% confidence interval of pre-stimulus, spontaneous firing rates. We quantified response magnitude as the total number of spikes exceeding the 95% confidence interval in the 100 ms after the stimulus onset divided by the total number of stimuli.

2.7. Anatomical tracing

We deeply anesthetized animals with isoflurane in a stereotaxic frame, and used a dental drill to expose the region over the parabrachial nucleus and over the middle meningeal artery. We used a glass pipette with a 40 μm tip to pressure inject (Nanoliter 2010 pump, World Precision Instruments, Sarasota, FL) 500 nL (50 nl/min) of CF568-conjugated cholera toxin B (CF568 conjugated CTB; Biotium, Fremont, CA) into PB unilaterally (right side). We made a craniotomy over the right middle meningeal artery and carefully exposed the dura, applying 5 μl of Fluorogold (Hydroxystilbamine FluoroGold, Biotium, Fremont, CA) to the area, diluted to 5% in sterile saline, using a sterile pipette tip. We covered the dura application site with sterile Gelfoam and closed the incision with nylon suture. One week after tracer application we deeply anesthetized the rat with urethane and performed a transcardial perfusion with 0.05 M PBS followed by 4% PFA (Sigma Millipore). We harvested the brains and trigeminal ganglia, placing them into 4% PFA overnight. We then transferred tissue to a solution of 30% sucrose in 0.05 M PBS, until the tissue blocks sank. We then froze the tissue (−20 °C) and used a cryostat (CM1860, Leica Biosystems, Buffalo Grove, IL) to section the PB injection site and the spinal trigeminal nucleus (positive control region) at 40 μm thickness. We sectioned the trigeminal ganglia on a cryostat at 30 μm thickness. We then rinsed all sections in 0.05 M PBS six times, before mounting the tissue on slides and coverslipping them for imaging. We searched for and imaged labeled cells using a Confocal Microscope (SP8, Leica Biosystems, Buffalo Grove, IL).

2.8. Statistical analysis

We analyzed all data using GraphPad PRISM version 8.2.0 for Macs (GraphPad Software, La Jolla, CA). When the assumptions necessary to use parametric tests were not met (normal distribution, independent data, and homogenous variance), we used non-parametric statistics. To determine age and sex differences we averaged values of each metric for an individual animal, such that n = the number of animals, and compared these averages between sexes or ages (2.5–3 months, 5–6 months or 8–12 months).

2.9. Rigor and reproducibility

We adhered to accepted standards for rigorous study design and reporting to maximize the reproducibility and translational potential of our findings as described by Landis et al. (Landis, 2012) and in ARRIVE (Animal Research: Reporting In Vivo Experiments).

3. Results

3.1. PB neurons respond to dura stimulation

We identified 58 PB neurons from 22 rats that responded to electrical stimulation of the dura mater. Responsive PB neurons were primarily located in the external lateral portion of PB (Fig. 1A). Fig. 1B depicts the action potential waveforms and the response patterns of two representative neurons. The peak response latency of PB responses to dura stimulation ranged from 4 ms to 25 ms (median 10 ms, 95% C.I. 8–12 ms), onset latency ranged from 4 ms to 20 ms (median 7 ms, 95% C.I. 7–8 ms), and rise time ranged from 0 ms to 11 ms (median 1 ms, 95% C.I. 1–2 ms) (Fig. 2A, B). Response magnitudes ranged from 0.02–2.5 spikes/stimulus (median 0.5 spikes/stimulus, 95% C.I. 0.28–0.80 spikes/stimulus) (Fig. 2D). The median spontaneous activity of these neurons was 0.72 Hz (95% C.I. 0.22–3.7). Thus, PB neurons respond reliably and with short latency to dura stimulation.

Because we recorded responses both ipsilateral (n = 17 neurons) and contralateral (n = 41 neurons) to dura stimulation, we compared response metrics based on stimulation localization. We found that ipsilateral stimulation elicited responses with shorter onset latency (Mann

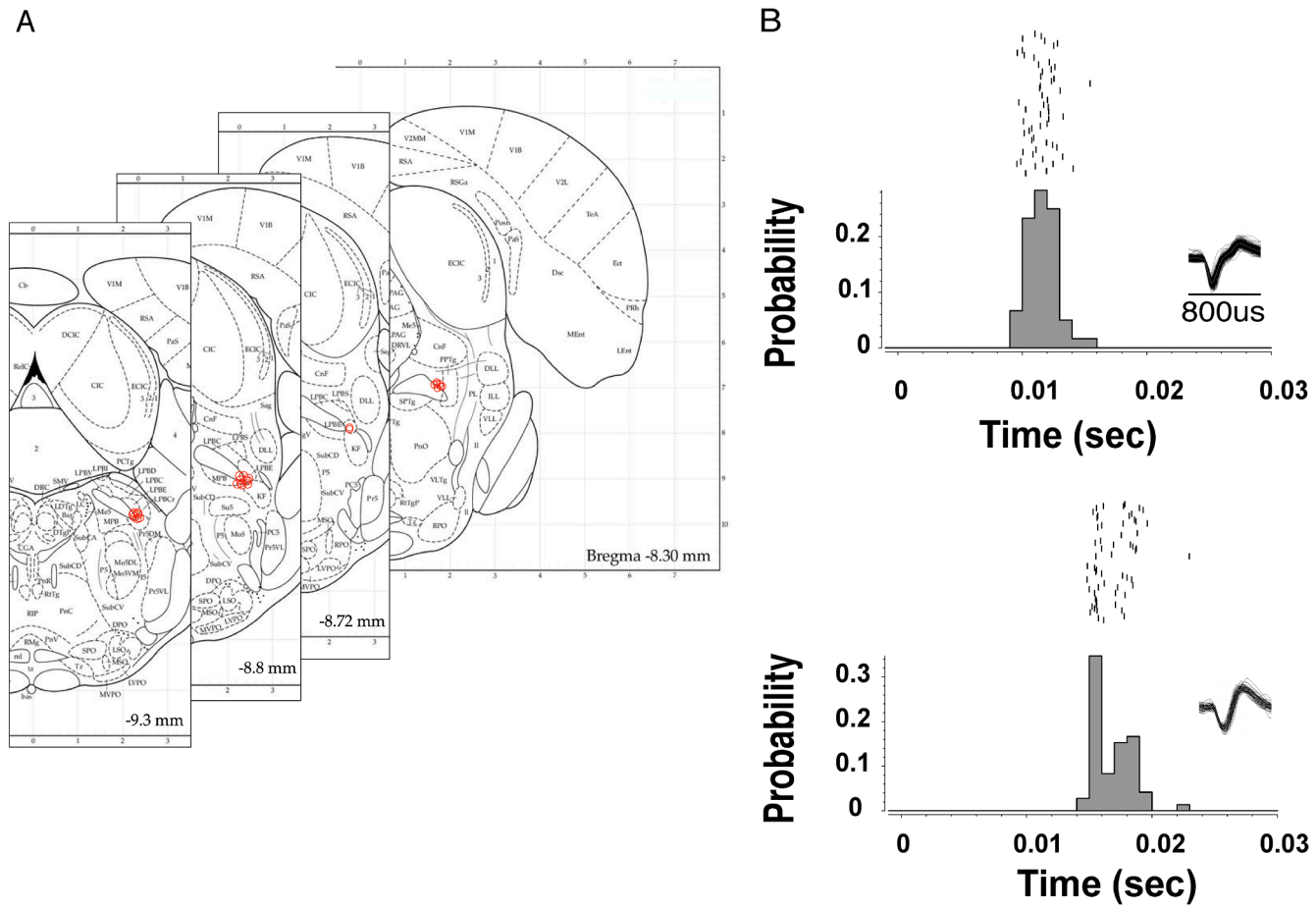

Fig. 1. (A) Neurons responding to dura stimulation are in the external lateral PB. Atlas plates[1] diagramming coronal sections of the rat brain, in the vicinity of PB. Red circles depict the coordinates of dura-responsive PB neurons. (B) PB neurons respond reliably to electrical dura stimulation. Two representative perievent rasters from dura-responsive PB neurons. Insets depict the waveform for each neuron. Stimulation onset is aligned to time zero. Rows of rasters above the histogram depict consecutive trials of dura stimulation. (1. Paxinos, G. & Watson, C. The rat brain in stereotaxic coordinates: hard cover edition (Elsevier, 2006).) (For interpretation of the references to colour in this figure legend, the reader is referred to the web version of this article).

Whitney U = 211, p = 0.02), shorter peak latency (Mann-Whitney U = 150, p = 0.0004) and shorter rise times (Mann-Whitney U = 205.5, p = 0.01). Response magnitudes were comparable between stimulation conditions (Ipsilateral stimulation: median onset latency 6 ms, 95% C.I. 6–7 ms, median peak latency 7 ms, 95% C.I. 7–8 ms, median rise time 1 ms, 95% C.I. 0–1 ms, median response magnitude 0.50 spikes/stimulus, 95% C.I. 0.28–0.88 spikes/stimulus. Contralateral stimulation: median onset latency 8 ms, 95% C.I. 7–10 ms, median peak latency 11 ms, 95% C.I. 10–14 ms, median rise time 2 ms, 95% C.I. 1–3 ms, median response magnitude 0.49 spikes/stimulus, 95% C.I. 0.19–0.82 spikes/stimulus).

There were no sex differences in peak latency (unpaired *t* test, t(18) = 0.57, p = 0.58), onset latency (unpaired *t* test, t(18) = 0.20, p = 0.84), rise time (Mann Whitney U = 48.5, p = 0.96), or response magnitude (Welch's *t* test, t(12.9) = 0.32, p = 0.75). Because we used rats at a range of ages for the electrophysiology experiments, we tested for age effects by dividing animals into 3 age groups: 2.5–3 months (9 rats), 5–6 months (5 rats), and 8–12 months (7 rats). There were no age differences in peak latency (Kruskal-Wallis statistic = 2.8, p = 0.26), onset latency (Kruskal-Wallis statistic = 2.9, p = 0.24), rise time (Kruskal-Wallis statistic = 2.4, p = 0.31), or response magnitude (Kruskal-Wallis statistic = 1.6, p = 0.47).

3.2. Dura- responsive PB neurons have diverse receptive fields

We mapped the receptive field of 48 of the 58 recorded neurons. Fig. 3 depicts the types of receptive fields we encountered. Most neurons responded only to dura stimulation, and not to noxious or innocuous tactile stimulation anywhere else on the body (28 neurons from both males and females ranging from 3 months to 12 months of age). Four neurons responded to noxious pinch on the hind-limbs bilaterally (from an 8-month old male and a 12-month old female), and two responded to pinch on the face bilaterally (from a 3-month old female and a 6-month-old female). One neuron responded to pinch on the hind-limb, fore-limbs, and face bilaterally (from an 8.5-month old male), while two neurons responded to pinch diffusely across the body, with the exception of the tail (from an 8-month old male and a 12-month old female). Eleven neurons responded to pinch across the entire body, including the tail (from two 6-month old males, an 8-month old male, a 3-month old female, a 6-month old female, and an 8-month old female). We carefully mapped the somatic receptive fields of each neuron with manually applied stimuli that did not produce a timestamp for stimulus onset. Therefore, we are unable to compute tactile response PSTHs. In our previous study, where we focused on PB responses to somatic inputs, we provide examples of such PSTHs (Uddin, 2018).

3.3. Trigeminal ganglion neurons innervating the dura and projecting to PB

After applying fluorescent retrograde tracers to PB and to the dura, we removed and sliced the trigeminal ganglion, examining tissue for evidence of tracer overlap (Fig. 4).

PB injection sites were located primarily in the lateral PB (Fig. 4A)

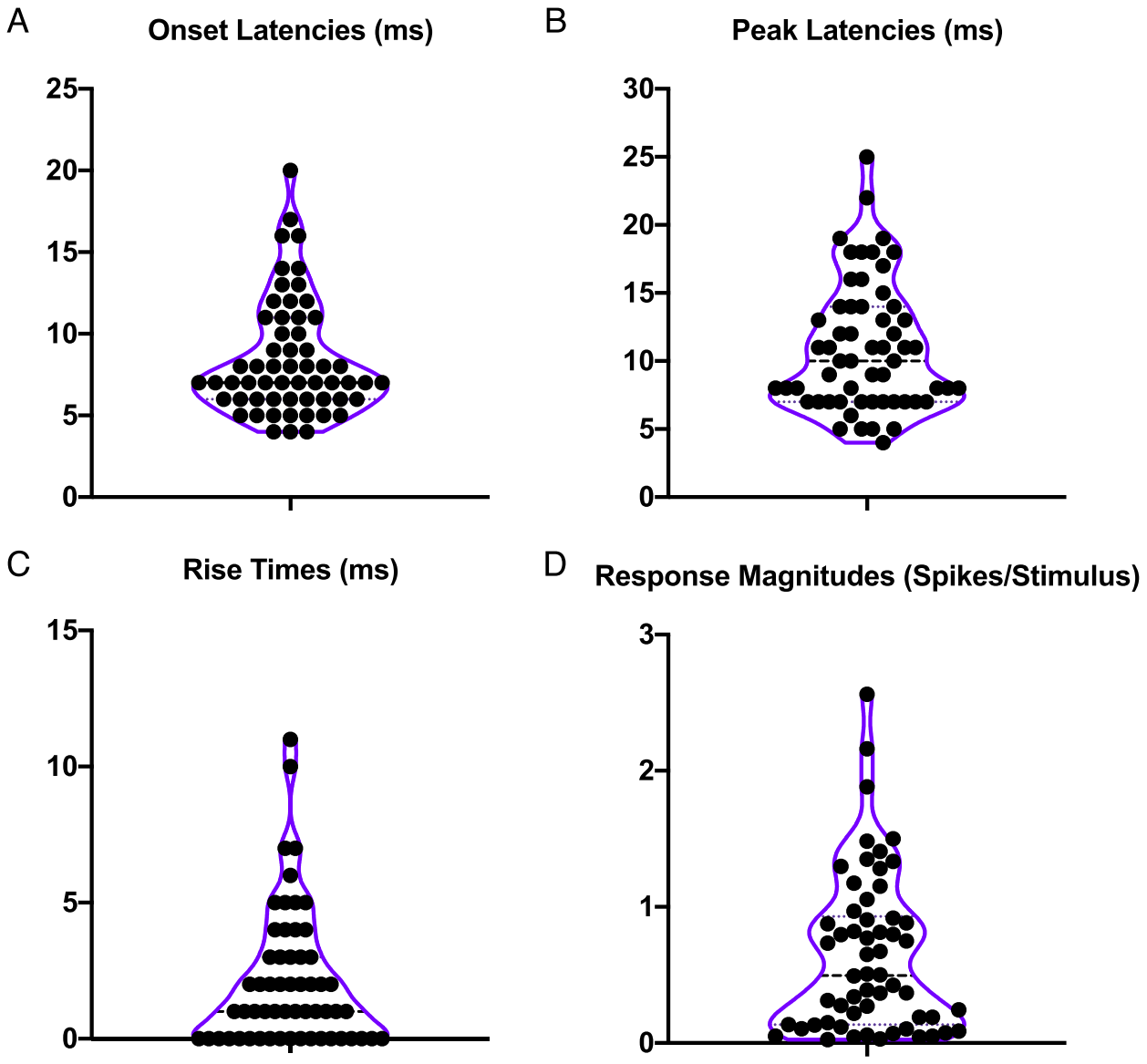

Fig. 2. PB neurons respond robustly and with short latency to dura stimulation. (A) The median onset latency is 7 ms (95% C.I. 7–8), (B) median peak latency is 10 ms (95% C.I. 8–12), (C) median rise time is 1 ms (95% C.I. 1–2). (D) Median response magnitude is 0.5 spikes/stimulus (95% C.I. 0.28–0.80 spikes/stimulus). For each panel, n = 58 neurons from 22 rats. Each data point represents data from one cell. Dotted horizontal lines depict medians and quartiles. Purple lines show the frequency distribution of the data. (For interpretation of the references to colour in this figure legend, the reader is referred to the web version of this article.)

and resulted in retrogradely-labeled CTB cell bodies in the spinal trigeminal nucleus caudalis and in the nucleus of the solitary tract, nuclei known to project to PB (Herbert et al., 1990; Saito, 2017). In the trigeminal ganglion we identified somata retrogradely labeled with Fluorogold which was placed on the dura, representing dura-projecting trigeminal afferents (Fig. 4C). We performed quantification in 3 animals, counting 550 FluoroGold positive neurons in 174 sections.

We also identified retrogradely-labeled neuronal somata in the trigeminal ganglion, consistent with a direct projection from the trigeminal ganglion to PB (Fig. 4C). In all animals examined, we identified neurons labeled for both CTB and Fluorogold, representing trigeminal neurons with peripheral axons that innervate the dura, and central axons that project directly to PB (Fig. 4C). Of the 550 Fluorogold positive cells counted, 26.3% (standard deviation 8.3%) were also CTB positive. Most Fluorogold labeled somata—representing dura projecting neurons—were interspersed between fiber tracts, presumably belonging to the ophthalmic branch of the trigeminal nerve. Double-labeled somata, representing neurons that innervate both the dura and PB, were located throughout regions containing somata labeled with only Fluorogold, without an obvious somatotopic organization.

4. Discussion

4.1. Dura-stimulus-responsive PB neurons

We report that PB neurons respond to inputs from the dura. We identified a subset of PB neurons that respond with short latencies to electrical stimulation of the dura mater. Although we initially surveyed coordinates throughout PB, the majority of responsive neurons were located in the lateral and external lateral portion of the complex, consistent with evidence of cFos activation in the lateral PB after dura irritation (Malick et al., 2001). Distinct subregions of PB can diverge

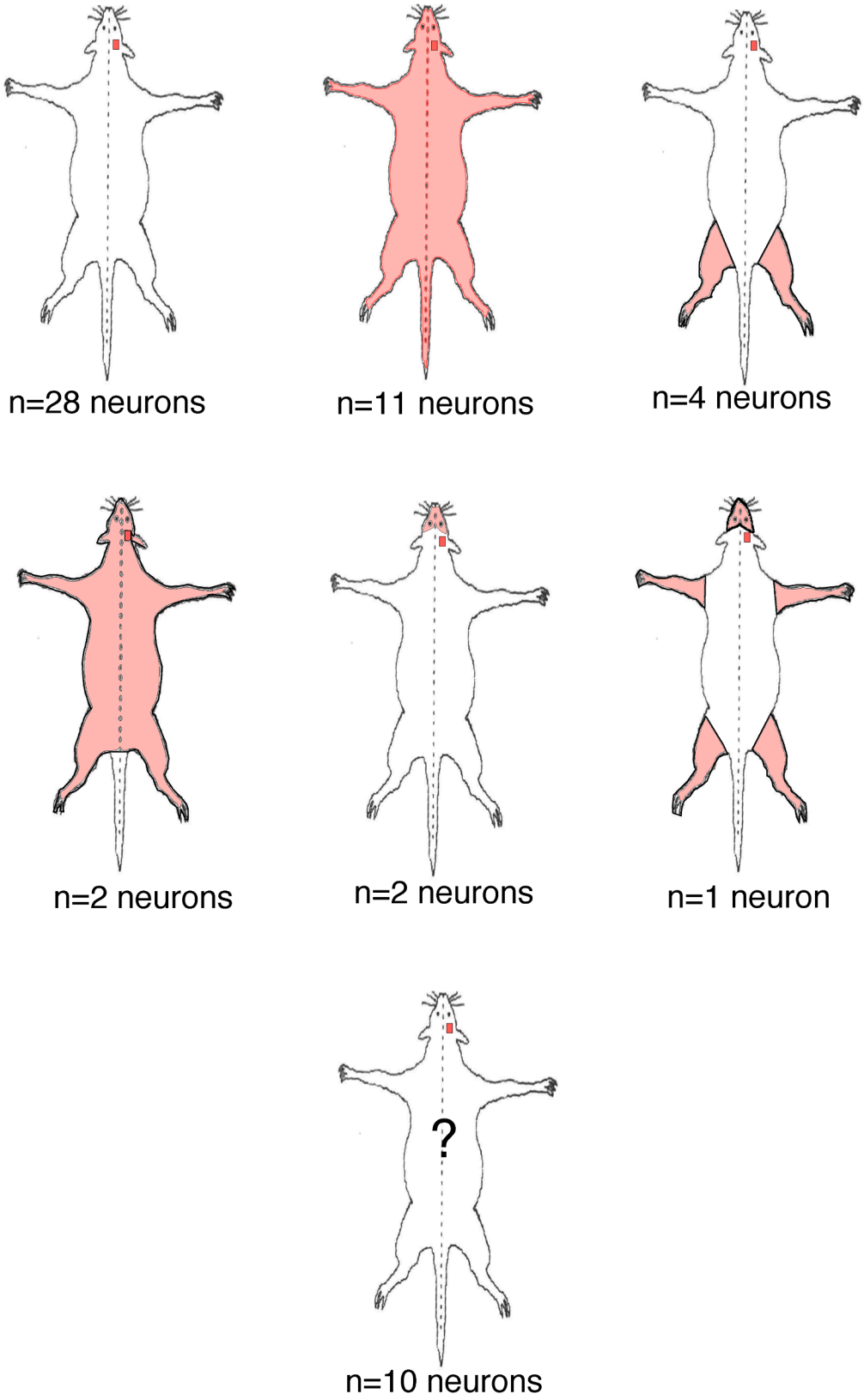

Fig. 3. Dura-responsive PB neurons have diverse receptive fields. The small red square represents responses to dura stimulation and pink shading shows the cutaneous receptive field. While most neurons responded only to dura stimulation (28/48), a significant proportion responded both to dura stimulation and to pinch across the entire body (pink shading: 11/48). A small number of neurons responded both to dura stimulation and to pinch on a more restricted receptive field, depicted by the pink shading (n = 9 total). We did not obtain receptive field information for 10 of the recorded neurons, denoted by the question mark on the final rat diagram. (For interpretation of the references to colour in this figure legend, the reader is referred to the web version of this article.)

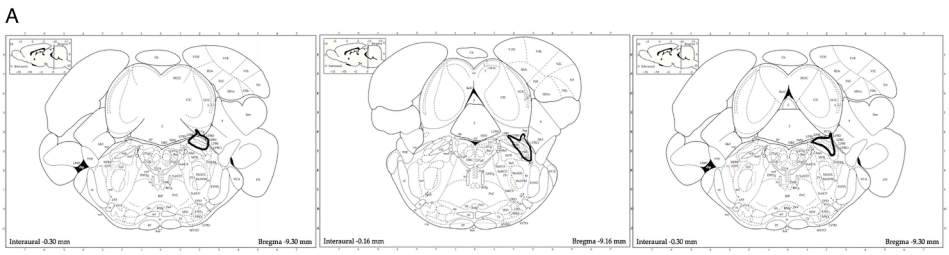

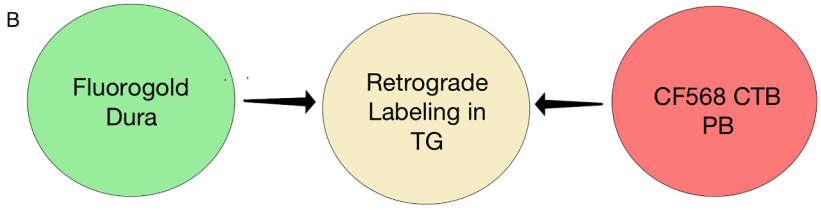

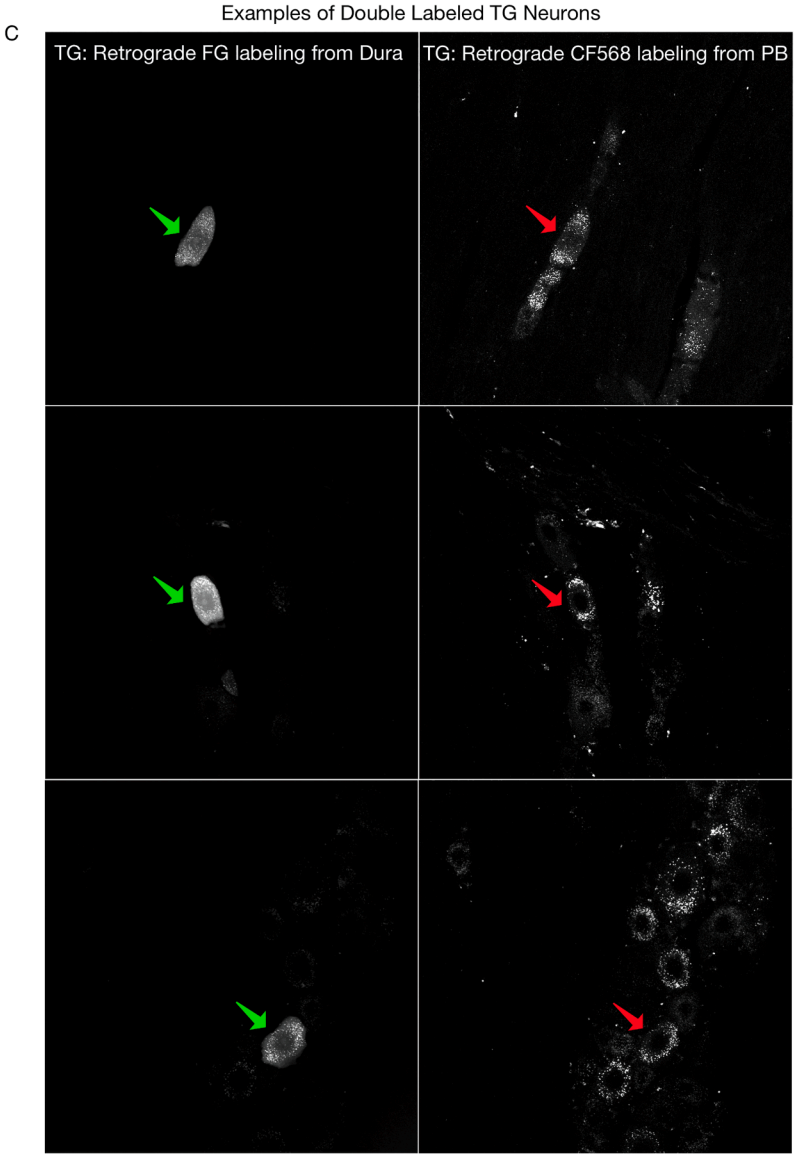

Fig. 4. Dura afferents project directly to PB. (A) A map of the injection site cores, depicted by black outlines. (B) The diagram depicts the experimental setup. CTB labels PB-projecting TG neurons and Fluorogold labels dura-innervating TG neurons. (C) Examples of dual-labeled neurons are representative images from 3 different animals – arrows denote double labeled cells. The green arrows indicate Fluorogold labeling and the red arrows indicate CTB labeling. Confocal images are shown in their native grayscale format. (For interpretation of the references to colour in this figure legend, the reader is referred to the web version of this article.)

anatomically and functionally, with the external lateral PB being particularly implicated in aversive learning (Chiang, 2020).

The majority of the neurons recorded responded only to dura stimulation, but a considerable number had extensive cutaneous receptive fields. These large receptive fields are consistent with prior reports, including ours, on PB responses (Uddin, 2018; Bester et al., 1995). Understanding the receptive fields of these dura-responsive PB neurons is important, because extra-cranial sensitivity—allodynia in particular—is associated with poor treatment response in patients with migraine (Burstein et al., 2004; Lipton, 2017; Louter, 2013). Here, we use electrical stimulation of the dura as a means of identifying PB neurons that encode dura inputs, not as a method of modeling migraine-associated dura irritation. Thus, further work is needed to clarify how dura responsive PB neurons with wide receptive fields might contribute to extra-cranial pain and allodynia in migraine model conditions.

The short-latency responses of PB neurons—particularly in response to ipsilateral dura stimulation—are consistent with monosynaptic connections between trigeminal ganglion neurons innervating the dura, and responsive PB neurons. The presence of responses to contralateral stimulation could represent an indirect pathway, but an alternative explanation is that these responses are also direct: while most trigeminal innervation of the dura mater arises from the ipsilateral ganglion, there have been reports of contralateral innervation and of trigeminal ganglion neurons innervating anatomically disparate regions of the dura (Keller et al., 1985; O'Connor and van der Kooy, 1986).

We do, however, recognize that these responses might also reflect a polysynaptic pathway, most likely *via* the spinal trigeminal nucleus caudalis, as there is a known anatomical connection from medullary trigeminal neurons to PB (Saito, 2017). Electrical stimulation of the dura activates medullary trigeminal neurons with an average latency of 11 ms (Strassman et al., 1986), which is longer compared to the median onset latency of 7 ms for PB neurons responsive to dura stimulation. While shorter latency responses can support the existence of a direct pathway, we acknowledge that response latency alone is not an adequate surrogate for the synaptic complexity of a pathway, especially when the conduction velocity of the axons involved is not conclusive (Berry and Pentreath, 1976). Future experiments investigating the effect of inactivating nodes along a potential indirect pathway, such as the spinal trigeminal nucleus, is necessary to establish whether the responses reported here are direct or indirect. Experiments such as these coupled with careful behavioral observations will also aid in determining the functional significance of the proposed anatomical pathway.

4.2. Anatomical evidence corroborating a direct trigeminal ganglion-to-PB pathway

Several studies suggested a direct connection between the trigeminal ganglion and the parabrachial complex, circumventing the canonical relay site in the spinal trigeminal nucleus (Panneton et al., 2006; Cavanaugh, 2011a, 2011b; Panneton and Gan, 2014). More recently, Rodriguez and colleagues demonstrated a monosynaptic, trigeminal ganglion to PB connection that is implicated in craniofacial pain (Rodriguez, 2017). In support of these findings, we demonstrate here retrogradely-labeled trigeminal ganglion neurons after injecting a tracer in PB. We acknowledge that spread of the injected tracer might lead to tracer uptake in neighboring regions, however, the core of the injection sites were centered in PB. These PB-projecting trigeminal ganglion neurons project also to the dura. Thus, these neurons represent a direct pathway between the dura, a structure implicated in migraine, and PB, a key node in chronic pain and aversion.

5. Conclusions

Here, we demonstrate short-latency responses to dura stimulation in lateral PB, suggesting a possible direct pathway between the trigeminal ganglion and PB. Anatomical evidence corroborates this finding, showing trigeminal ganglion neurons that project peripherally to dura and centrally to PB. Given PB's critical role in maladaptive pain conditions, this pathway is important for further study in the context of migraine pain.

Funding sources

This work was supported by the National Institutes of Health (R01NS099245 and R01NS069568).

CRediT authorship contribution statement

Olivia Uddin: Conceptualization, Investigation, Formal analysis, Writing - review & editing. **Michael Anderson:** Investigation, Writing - review & editing. **Jesse Smith:** Investigation, Writing - review & editing. **Radi Masri:** Conceptualization, Funding acquisition, Writing - review & editing. **Asaf Keller:** Conceptualization, Investigation, Funding acquisition, Formal analysis, Writing - review & editing, Supervision.

Conflicts of Interest

The authors declare that there is no conflict of interest regarding the publication of this paper.

References

Berry, M.S., Pentreath, V.W., 1976. Criteria for distinguishing between monosynaptic and polysynaptic transmission. Brain Res. 105, 1–20.
Bester, H., Menendez, L., Besson, J.M., Bernard, J.F., 1995. Spino (trigemino) parabrachiohypothalamic pathway: electrophysiological evidence for an involvement in pain processes. J. Neurophysiol. 73, 568–585.
Bianchi, R., Corsetti, G., Rodella, L., Tredici, G., Gioia, M., 1998. Supraspinal connections and termination patterns of the parabrachial complex determined by the biocytin anterograde tract-tracing technique in the rat. J. Anat. 193, 417–430.
Bigal, M.E., et al., 2008. Prevalence and characteristics of allodynia in headache sufferers: a population study. Neurology 70, 1525–1533.
Burch, R., Rizzoli, P., Loder, E., 2018. The prevalence and impact of migraine and severe headache in the United States: figures and trends from Government Health Studies. Headache 58, 496–505.
Burgos-Vega, C.C., et al., 2019. Non-invasive dural stimulation in mice: a novel preclinical model of migraine. Cephalalgia 39, 123–134.
Burstein, R., Yamamura, H., Malick, A., Strassman, A.M., 1998. Chemical stimulation of the intracranial dura induces enhanced responses to facial stimulation in brain stem trigeminal neurons. J. Neurophysiol. 79, 964–982.
Burstein, R., Yarnitsky, D., Goor-Aryeh, I., Ransil, B.J., Bajwa, Z.H., 2000. An association between migraine and cutaneous allodynia. Ann. Neurol. 47, 614–624.
Burstein, R., Collins, B., Jakubowski, M., 2004. Defeating migraine pain with triptans: a race against the development of cutaneous allodynia. Ann. Neurol. 55, 19–26.
Campos, C.A., Bowen, A.J., Roman, C.W., Palmiter, R.D., 2018. Encoding of danger by parabrachial CGRP neurons. Nature 555, 617–622.
Cavanaugh, D.J., et al., 2011. Restriction of transient receptor potential vanilloid-1 to the peptidergic subset of primary afferent neurons follows its developmental downregulation in nonpeptidergic neurons. J. Neurosci. 31, 10119–10127.
Cavanaugh, D.J., et al., 2011. Trpv1 reporter mice reveal highly restricted brain distribution and functional expression in arteriolar smooth muscle cells. J. Neurosci. 31, 5067–5077.
Chiang, M.C., et al., 2019. Parabrachial complex: a hub for pain and aversion. J. Neurosci. 39, 8225–8230.
Chiang, M.C., et al., 2020. Divergent neural pathways emanating from the lateral parabrachial nucleus mediate distinct components of the pain response. Neuron.
Davern, P.J., 2014. A role for the lateral parabrachial nucleus in cardiovascular function and fluid homeostasis. Front. Physiol. 5, 436.
Dodick, D.W., 2018. Migraine. Lancet 391, 1315–1330.
Fontaine, D., et al., 2018. Dural and pial pain-sensitive structures in humans: new inputs from awake craniotomies. Brain 141, 1040–1048.
Friedberg, M.H., Lee, S.M., Ebner, F.F., 1999. Modulation of receptive field properties of thalamic somatosensory neurons by the depth of anesthesia. J. Neurophysiol. 81, 2243–2252.
Gauriau, C., Bernard, J.F., 2002. Pain pathways and parabrachial circuits in the rat. Exp. Physiol. 87, 251–258.
Hajnal, A., Norgren, R., Kovacs, P., 2009. Parabrachial coding of sapid sucrose: relevance to reward and obesity. Ann. NY. Acad. Sci. 1170, 347–364.
Headache Classification Committee of the International Headache Society (IHS), 2018. The International Classification of Headache Disorders, 3rd edition. Cephalalgia 38, 1–211.
Herbert, H., Moga, M.M., Saper, C.B., 1990. Connections of the parabrachial nucleus with the nucleus of the solitary tract and the medullary reticular formation in the rat. J. Comp. Neurol. 293, 540–580.

Jergova, S., Kolesar, D., Cizkova, D., 2008. Expression of c-Fos in the parabrachial nucleus following peripheral nerve injury in rats. Eur. J. Pain 12, 172–179.
Keller, J.T., Saunders, M.C., Beduk, A., Jollis, J.G., 1985. Innervation of the posterior fossa dura of the cat. Brain Res. Bull. 14, 97–102.
Krukoff, T.L., Harris, K.H., Jhamandas, J.H., 1993. Efferent projections from the parabrachial nucleus demonstrated with the anterograde tracer Phaseolus vulgaris leucoagglutinin. Brain Res. Bull. 30, 163–172.
Landis, S.C., et al., 2012. A call for transparent reporting to optimize the predictive value of preclinical research. Nature 490, 187.
Lipton, R.B., et al., 2017. Allodynia is associated with initial and sustained response to acute migraine treatment: results from the American Migraine Prevalence and Prevention Study. Headache 57, 1026–1040.
Louter, M.A., et al., 2013. Cutaneous allodynia as a predictor of migraine chronification. Brain 136, 3489–3496.
Malick, A., Jakubowski, M., Elmquist, J.K., Saper, C.B., Burstein, R., 2001. A neurohistochemical blueprint for pain-induced loss of appetite. Proc. Natl. Acad. Sci. U.S.A. 98, 9930–9935.
Martelli, D., Stanić, D., Dutschmann, M., 2013. The emerging role of the parabrachial complex in the generation of wakefulness drive and its implication for respiratory control. Respir. Physiol. Neurobiol. 188, 318–323.
Matsumoto, N., Bester, H., Menendez, L., Besson, J.M., Bernard, J.F., 1996. Changes in the responsiveness of parabrachial neurons in the arthritic rat: an electrophysiological study. J. Neurophysiol. 76, 4113–4126.
Moskowitz, M.A., 1984. The neurobiology of vascular head pain. Ann. Neurol. 16, 157–168.
Noseda, R., Burstein, R., 2013. Migraine pathophysiology: anatomy of the trigeminovascular pathway and associated neurological symptoms, CSD, sensitization and modulation of pain. Pain 154 (Suppl. 1).
O'Connor, T.P., van der Kooy, D., 1986. Pattern of intracranial and extracranial projections of trigeminal ganglion cells. J. Neurosci. 6, 2200–2207.
Oshinsky, M.L., Gomonchareonsiri, S., 2007. Episodic dural stimulation in awake rats: a model for recurrent headache. Headache 47, 1026–1036.
Panneton, W.M., Gan, Q., 2014. Direct reticular projections of trigeminal sensory fibers immunoreactive to CGRP: potential monosynaptic somatoautonomic projections. Front. Neurosci. 8, 136.
Panneton, W.M., Gan, Q., Juric, R., 2006. Brainstem projections from recipient zones of the anterior ethmoidal nerve in the medullary dorsal horn. Neuroscience 141, 889–906.
Raver, C., et al., 2020. An amygdalo-parabrachial pathway regulates pain perception and chronic pain. J. Neurosci. 40, 3424–3442.
Rodriguez, E., et al., 2017. A craniofacial-specific monosynaptic circuit enables heightened affective pain. Nat. Neurosci. 20, 1734–1743.
Roeder, Z., et al., 2016. Parabrachial complex links pain transmission to descending pain modulation. Pain 157, 2697–2708.
Saito, H., et al., 2017. Ascending projections of nociceptive neurons from trigeminal subnucleus caudalis: a population approach. Exp. Neurol. 293, 124–136.
Spike, R.C., Puskar, Z., Andrew, D., Todd, A.J., 2003. A quantitative and morphological study of projection neurons in lamina I of the rat lumbar spinal cord. Eur. J. Neurosci. 18, 2433–2448.
Strassman, A., Mason, P., Moskowitz, M., Maciewicz, R., 1986. Response of brainstem trigeminal neurons to electrical stimulation of the dura. Brain Res. 379, 242–250.
Strassman, A.M., Raymond, S.A., Burstein, R., 1996. Sensitization of meningeal sensory neurons and the origin of headaches. Nature 384, 560–564.
Uddin, O., et al., 2018. Amplified parabrachial nucleus activity in a rat model of trigeminal neuropathic pain. Neurobiol. Pain 3, 22–30.